

Comparison of Algorithms for Intensity Modulated Beam Optimization: Projections Onto Convex Sets and Simulated Annealing

Paul S. Cho, Shinhak Lee, Robert J. Marks II, Joshua A. Redstone, and Seho Oh

University of Washington, Seattle, WA 98195-6043

We describe a new class of optimization method based on the theory of alternating projections onto convex sets (POCS). The technique is applied to the problem of intensity modulated beam optimization in conformal radiotherapy. The results of test cases are compared with those from a well established method of simulated annealing.

THE METHOD OF POCS

The theory of POCS is due to Bregman [1] and Gubin [2] and was advanced by Youla [3] and Stark [4]. For biomedical applications POCS has been applied to the problem of incomplete projection data in computerized tomography [5].

POCS is constructed around constraint sets. A set C is convex if $\bar{x}_1 \in C$ and $\bar{x}_2 \in C$ implies that

$$\alpha\bar{x}_1 + (1-\alpha)\bar{x}_2 \in C \quad (1)$$

for all $0 \leq \alpha \leq 1$. Geometrically, as illustrated in Figure 1, this means that the line segment connecting \bar{x}_1 and \bar{x}_2 is totally subsumed in the set C . Therefore, the set in (a) is convex while the set shown in (b) is not convex since there are elements in \bar{x}_1 and \bar{x}_2 that produce a line segment that partially lies outside of the set.

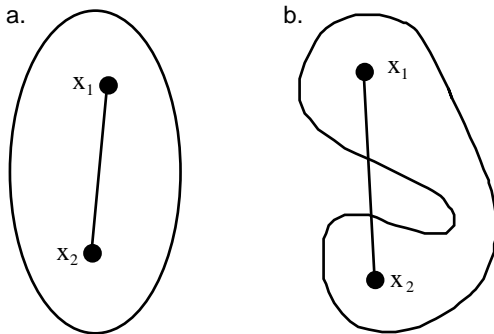


Figure 1. Illustration of (a) convex and (b) non-convex set.

Given two or more convex sets, successive projection of normal vectors with respect to each set will find the intersection which satisfies all the constraints as shown in Figure 2.

POCS assumes that the convex constraint sets intersect. If the sets share a single intersection, there exists a unique solution which satisfies all the constraints. If the intersection consists of many points, the solution is determined by such factors as the initialization process. On the other hand, if the sets do not intersect, there is no solution that satisfies the constraints. In practice, non-intersecting constraint sets could occur if the dose prescription is too stringent or unrealistic.

It can be shown that the constraints commonly used in radiotherapy treatment planning are convex [6]. These constraints include target dose uniformity, upper limit on normal tissue dose, and

non-negativity of radiation fluence. For example, consider possible dose distributions within a critical organ which are required to remain below 30 Gy. In this case the doses between 0 and 30 Gy comprise the constraint set. The set is convex if it satisfies the condition given by equation (1). The fact that this is indeed the case is easily seen by noting that any linear combination of doses between 0 and 30 Gy also lies within the set. Taking a most extreme case, for instance, if two members of the set $D_1 = 29.9$ Gy and $D_2 = 29.8$ Gy, then the necessary condition $\alpha D_1 + (1-\alpha)D_2 < 30$ Gy is true for all $0 \leq \alpha \leq 1$. Therefore, the organ dose constraint can be expressed as a convex set. Mathematical proofs of convexity of radiotherapy constraints are given in [6].

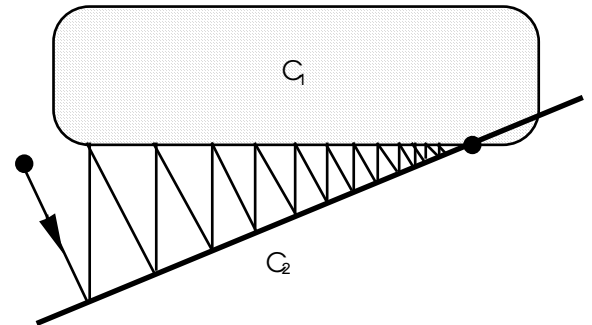


Figure 2. Successive projections between two convex sets resulting in convergence to a fixed point.

The dosimetric frame work for application of POCS in radiotherapy assumes the form

$$\bar{d}_k = \mathbf{A}_k \bar{b}_k \quad (2)$$

where \bar{d}_k is the dose vector for the k -th beam, \mathbf{A}_k is a dose computation matrix which provides the values of fractional dose contribution to a sample point from a beam element, and \bar{b}_k is an array of pencil beam weights for the k -th beam.

For inverse dose computation \bar{d}_k is the prescribed dose distribution, \mathbf{A}_k is computed using a photon transport algorithm of choice, and \bar{b}_k is the unknown. As a rule, POCS projections must occur within the same domain. We have chosen the dose vector domain because the convex constraint sets are formulated most easily in this space.

Projection operators are formulated in such a way that the distance between a dose vector and its projection is minimized. For instance, the projection onto the target dose constraint is determined by finding the minimum of

$$J = \frac{1}{2} \sum_{k=1}^Q \|\vec{z}_k - d_k\|^2 + \lambda^T \mathbf{I}_T \left(\sum_{k=1}^Q z_k - p \right) \quad (3)$$

where \vec{z}_k is the projection vector, $\lambda^T \mathbf{I}_T$ is a spatial discriminator for the target volume, Q is the number of beams, and p is the prescription dose. Differentiating J with respect to \vec{z}_k and setting it to zero, the projection operator for the target dose constraint set is found:

$$P_T(d_k) = d_k + \frac{1}{Q} \mathbf{I}_T \left(p - \sum_{i=1}^Q d_i \right). \quad (4)$$

APPLICATION OF POCS IN INTENSITY MODULATED BEAM OPTIMIZATION

The method of POCS was applied to several different test cases with the number of beams ranging from 3 to 72. Figure 3 shows one of the test cases consisting of a crescent shaped tumor surrounding a critical organ. Dose contributions from pencil beams were precomputed using TPR for an 18-MV machine.

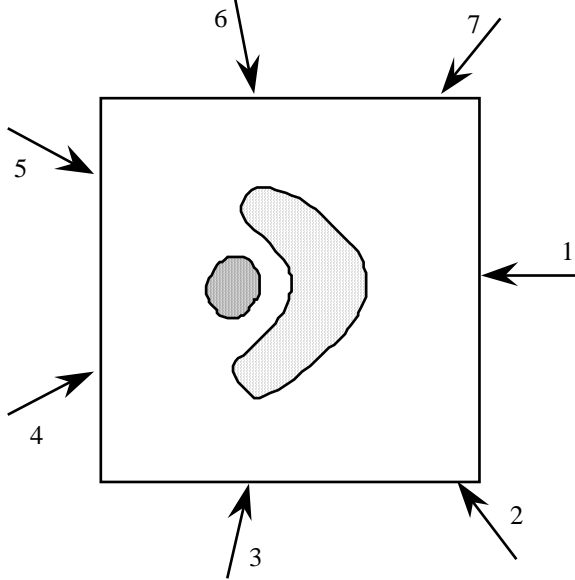


Figure 3. Crescent shape target and critical organ.

The following constraint sets were used:

- Target dose uniformity
- Normal tissue upper dose limit
- Non-negative beam weights
- Beam-dose relationship

POCS will converge even when some projections are used more than others. This property can be exploited to accelerate the convergence speed. For example, we achieved faster convergence by more frequently projecting between the beam-dose constraint set and the target uniformity set since projections between these sets are less computationally intensive than others. The POCS iteration was terminated when the difference between the prescribed and the calculated dose became sufficiently small.

The POCS optimization results using 7 beams discretized to 25 beam elements are shown in Figure 4. The target dose prescription was set to 100% while the critical organ dose was required to be less than or equal to 40% of the prescription. The dose volume histograms for varying number of POCS iterations indicate that the

target dose uniformity improves rapidly with iteration reaching the maximum at about 30 iterations.

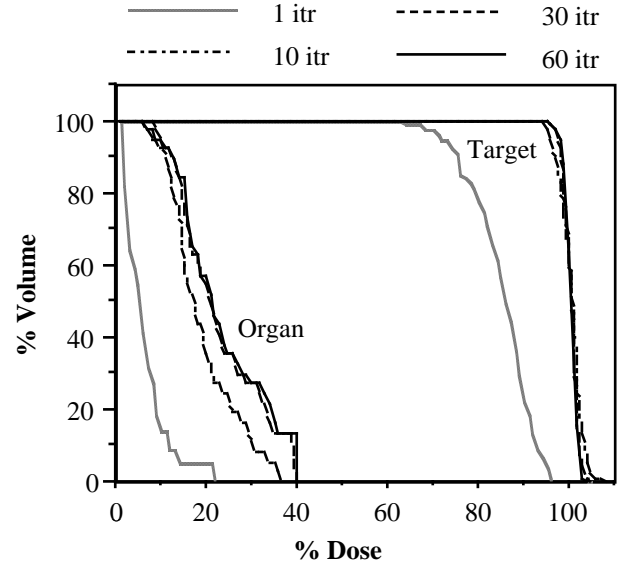


Figure 4. POCS optimization results presented in dose volume histograms for target and organ volumes. Number of iterations ranges from 1 to 60.

COMPARISON WITH SIMULATED ANNEALING

Since, in general, there are no unique solutions for the class of optimization problem with which we are dealing, the performance of a given algorithm can only be evaluated in comparison to other methods. The results of POCS optimization were compared with those from a simulated annealing method which has been established as a standard in radiotherapy treatment plan optimization. The fast simulated annealing (FSA) method was used to minimize the cost function

$$F = \sum_{i \in \text{target}} (D_i - P)^2 + \sum_{j=1}^N r_j O_j \quad (5)$$

where D_i is the dose to a sample point within the target, P is the prescribed dose, O_j is the penalty function for the normal structure j given by

$$O_j = \begin{cases} \sum_{k \in \text{organ}} (D_k - U_j)^2 & \text{for } D_k \geq U_j \\ \sum_{k \in \text{organ}} D_k & \text{for } D_k < U_j \end{cases} \quad (6)$$

where U_j is the upper dose limit imposed on the normal structure.

The simulated annealing method was applied to the beam optimization problem defined in Figure 3 using the same dose computation matrix. The initial width of Cauchy distribution, initial temperature, and the control parameters for the Cauchy generator and the temperature updating were optimized through systematic tuning. They were set to 0.16 (of the prescribed dose), 0.01, 2,000, and 4,000, respectively. A generous number of iterations were allowed in order to ensure convergence to a solution. The cost function values were monitored up to 500,000 iterations. The best cost occurred at about 200,000 iterations.

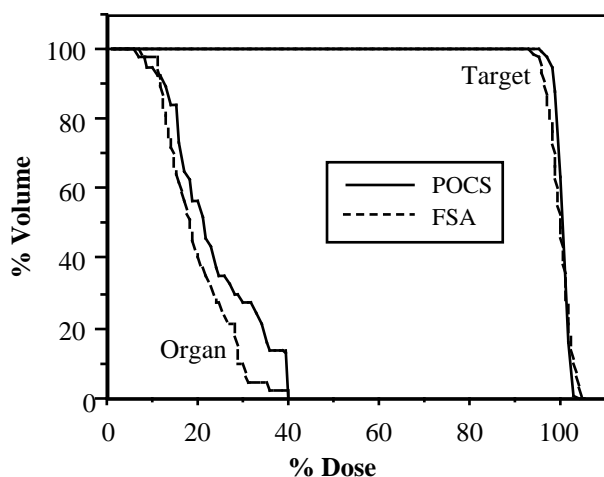


Figure 5. Comparison of POCS and FSA.

Figure 5 compares the POCS and FSA results after 60 and 200,000 iterations, respectively. Statistics on the target volume coverage are tabulated in Table 1. The POCS algorithm produced a higher minimum target dose (95%) than the simulated annealing method (93%). The target dose uniformity was also higher for POCS ($\sigma = 1.4\%$ vs. 2.5%). Both algorithms were able to satisfy the upper dose limit on the critical organ. The integrated organ dose was slightly lower for the simulated annealing which accounts for the loss in target dose uniformity. Had a different cost function other than the quadratic formulation been used, the performance might have matched the POCS more closely.

Table 1. Target dose distribution

	Min	Max	Mean	σ
POCS	95%	103%	99.9%	1.4%
FSA	93%	104%	99.9%	2.5%

The relative beam weights were plotted against the pencil beam position. Figure 6 is a comparison of beam profiles obtained by the two method for the beam angle 1 of Figure 3. It can be seen that the POCS method generates intensity modulation profiles which generally correspond to the prescribed dose distribution in the treatment geometry. This is a natural consequence of the projection operation which essentially forces the individual beam weights to be proportional to the associated line integrals through the dose distribution. On the other hand, due to its random nature in adjusting the beam weights, the simulated annealing method has the tendency to produce an intensity modulation that fluctuates independently of the tumor-organ shape. Less jagged fluence profiles are easier to deliver by the multileaf collimators and therefore are more desirable.

DISCUSSION

The method of POCS is substantially different from other optimization methods used in radiotherapy. Unlike most other techniques POCS does not rely on minimization of cost function. Instead, it seeks to find a solution which simultaneously satisfies specified constraints. As such, there is no concept of local minima in POCS. Feasibility of its use is determined by whether convex formulation exists for a given problem.

We have demonstrated that it is possible to formulate the constraints commonly used in radiotherapy in convex sets. The number of POCS iterations required for convergence is comparable to those

of other deterministic optimization methods, and compared to simulated annealing orders of magnitude less.

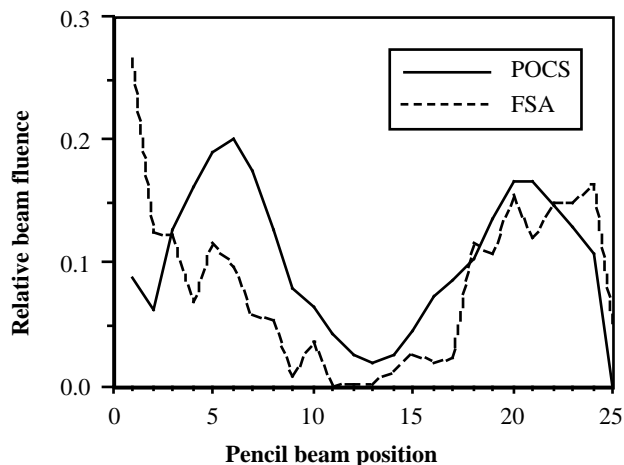


Figure 6. Comparison of beam profiles for the beam angle #1.

The results indicate that more uniform target dose distributions were obtained with the POCS method as compared with the simulated annealing technique using a quadratic objective function. Also it was noted that the beam intensity profiles generated by the POCS method correspond more closely to the target-organ geometry than those produced by the simulated annealing method.

While the constraints used in the illustration were simple, more complex constraints including dose-volume restrictions on normal tissues can be implemented [7].

REFERENCES

1. L.M. Bregman, "Finding the common point of convex sets by the method of successive projections," *Dokl. Akad. Nauk. USSR* **162**:487-490, 1965.
2. L.G. Gubin, B.T. Polyak and E.V. Raik, "The method of projections for finding the common point of convex sets," *USSR Comput. Math. Phys.* **7**:1-24, 1967.
3. D.C. Youla and H. Webb, "Image restoration by the method of convex projections: Part I-Theory," *IEEE Trans. Med. Imag.* **MI-1**:81-94, 1982.
4. H. Stark, *Image Recovery: Theory and Application*, Academic Press, Orlando, 1987.
5. M.I. Sezan and H. Stark, "Tomographic image reconstruction from incomplete view data by convex projections and direct Fourier inversion," *IEEE Trans. Med. Imag.* **MI-3**:91-98, 1984.
6. S. Lee, P.S. Cho, R.J. Marks II and S. Oh, "Conformal radiotherapy computation by the method of alternating projections onto convex sets," *Phys. Med. Biol.* (in press) 1997.
7. P.S. Cho, S. Lee, R.J. Marks II, S. Oh, S.G. Sutlief and M.H. Phillips, "Optimization of intensity modulated beams with volume constraints using two methods: cost function minimization and projections onto convex sets," *Med. Phys.* (submitted) 1997.